WISC

UNIVERSITY OF WISCONSIN • MADISON, WISCONSIN

PLASMA PHYSICS

STRONG RADIAL ELECTRIC FIELD SHEAR AND REDUCED FLUCTUATIONS IN A REVERSED-FIELD PINCH

39
5-27-97 JS ①

B.E. Chapman, C.-S. Chiang, S.C. Prager,
J.S. Sarff, and M.R. Stoneking

DOE/ER/54345-287 May 1997

ONSIN

NOTICE

This report was prepared as an account of work sponsored by an agency of the United States Government. Neither the United States nor any agency thereof, nor any of their employees, makes any warranty, expressed or implied, or assumes any legal liability or responsibility for any third party's use or the results of such use of any information, apparatus, product or process disclosed in this report, or represents that its use by such third party would not infringe privately owned rights.

Printed in the United States of America
Available from
National Technical Information Service
U.S. Department of Commerce
5285 Port Royal Road
Springfield, VA 22161

NTIS Price codes
Printed copy: A02
Microfiche copy: A01

DISCLAIMER

Portions of this document may be illegible in electronic image products. Images are produced from the best available original document.

Strong radial electric field shear and reduced fluctuations in a reversed-field pinch

B. E. Chapman, C.-S. Chiang, S. C. Prager, J. S. Sarff, and M. R. Stoneking

Department of Physics, University of Wisconsin, Madison, Wisconsin 53706

(Received

A strongly sheared radial electric field is observed in enhanced confinement discharges [Phys. Plasmas **3**, 709 (1996)] in the MST reversed-field pinch. The strong shear develops in a narrow region in the plasma edge. Electrostatic fluctuations are reduced over the entire plasma edge with an extra reduction in the shear region. Magnetic fluctuations, resonant in the plasma core but global in extent, are also reduced. The reduction of fluctuations in the shear region is presumably due to the strong shear, but the causes of the reductions outside this region have not been established.

PACS numbers: 52.55.Hc, 52.25.Fi, 52.25.Gj, 52.35.Qz

MASTER

DISTRIBUTION OF THIS DOCUMENT IS UNLIMITED

The reversed-field pinch (RFP) is a magnetically confined toroidal plasma configuration characterized by a relatively weak toroidal magnetic field whose direction in the plasma edge is opposite that in the core. There is also a poloidal magnetic field whose strength is comparable to that of the toroidal field. Fluctuations in the magnetic field have been measured to drive particle [1] and energy [2] transport in the plasma core, and reduction of magnetic fluctuations has been linked to recent improvements in particle and energy confinement [3,4]. Fluctuations in the electric field, induced by charge buildup in the plasma, have been measured to drive particle transport in the plasma edge [5], but the mechanism underlying energy transport in the edge has not been established. In general, magnetic fluctuations are believed to play a larger role than electrostatic fluctuations in determining RFP global transport.

In contrast to the RFP is the tokamak configuration, which has a strong, stabilizing toroidal magnetic field and weak magnetic fluctuations. Electrostatic fluctuations are believed to drive the bulk of particle and energy transport in the tokamak. In this (and other magnetic configurations) electrostatic fluctuations and transport have been reduced by the generation of strongly sheared $\boldsymbol{E} \times \boldsymbol{B}$ plasma flow attributed to shear in the radial electric field [6,7].

In this Letter, we report observations of a strongly sheared radial electric field in the RFP. The shear develops in a narrow region in the edge of enhanced confinement discharges, where the energy confinement time can reach triple the normal value [8]. Also observed in these discharges is a reduction of electrostatic

fluctuations over the entire plasma edge with an extra reduction in the shear region. These reductions occur over a broad range of frequencies. Magnetic fluctuations, resonant in the core but global in extent, are also reduced. The reduction of fluctuations in the shear region is presumably due to the strong shear, but the causes of the reductions outside this region have not been determined. Also yet to be determined is the relative contribution to enhanced confinement from each fluctuation reduction.

A distinguishing feature of these discharges is the reduction of low frequency fluctuations in the shear region. These fluctuations have correlation lengths substantially larger than the width of this region. This suggests that localized shear flow may influence non-localized fluctuations, unlike the standard tokamak case, where only small-scale fluctuations in and around the shear region are affected by the shear.

These observations were made in the Madison Symmetric Torus (MST) [9] RFP. The MST is a relatively large Ohmically heated device with a major radius of 150 cm and a minor radius of 52 cm. Graphite limiters mounted on the plasma-facing wall restrict the plasma minor radius to $\leq$ 51 cm. Subject to constraints on toroidal field reversal, electron density, wall conditioning, and fueling, enhanced confinement discharges are achievable at all plasma currents of which the MST is capable (100 kA $\leq I_\phi \leq$ 600 kA). The most important requirements are sufficiently strong toroidal field reversal and sufficiently low density. The toroidal field reversal is represented by $F \equiv B_t(a)/\langle B_t \rangle$, where $B_t(a)$ is the toroidal field at the edge, and $\langle B_t \rangle$ is the cross-section average. The reversal and

density requirements relax with increasing I_ϕ. For example, at 200 kA, the minimum (least negative) $F \sim -0.5$, and the maximum line-averaged density, $\langle n_e \rangle \sim 6 \times 10^{12}$ cm^{-3}. At 500 kA, the minimum $F \sim -0.2$, and the maximum $\langle n_e \rangle \sim 1.2 \times 10^{13}$ cm^{-3}. Enhanced confinement discharges requiring strong toroidal field reversal were also observed in the TPE-1RM20 RFP [10]. Discharges in this device exhibited reduced magnetic fluctuations, but neither electrostatic fluctuations nor the radial electric field were measured.

Careful conditioning of the plasma-facing wall is important as well. Enhanced confinement discharges were first obtained following boronization [8,11] but are now achievable with more standard wall conditioning techniques such as pulsed discharge cleaning in helium. Both the fuel and the fueling method are also important. Deuterium generally provides better confinement and reproducibility than hydrogen, and wall fueling is preferred over gas puff fueling. Wall fueling is achieved by turning off the puff valves after formation of the discharge, allowing the wall (including the limiters) to provide the necessary fuel through recycling and other processes.

To illustrate the differences between standard (low) and enhanced confinement, we compare two discharges in Fig. 1. The central electron temperature, indicated roughly by soft x-ray emission, is shown in Figs. 1(a) and 1(e), and the Ohmic input power is shown in Figs. 1(b) and 1(f). The emission from one impurity species in the plasma edge is shown in Figs. 1(c) and 1(g). Brief periods of enhanced confinement occur in both discharges around 10 ms. Shortly after 10 ms, these enhanced confinement periods are

interrupted by sawtooth crashes [8,12], where the central electron temperature decreases, and both the Ohmic input power and impurity radiation increase. The discharge on the left then degrades to standard confinement, while the discharge on the right exhibits a sustained period of enhanced confinement. With enhanced confinement, the central electron temperature is higher, and the Ohmic input power is lower. Radiation power loss from edge impurities is also reduced, as is the radiation from neutral fuel atoms (H_α, not shown). Both of these discharges satisfy all of the externally controllable conditions for enhanced confinement described above. Thus, while meeting these conditions is necessary, it is not always sufficient.

Due to the increase in stored thermal energy and the reduction of Ohmic input power, the enhanced energy confinement time, $\tau_E \equiv$ (stored thermal energy)/(Ohmic input power) is $\geq$ 3 ms, a roughly three-fold improvement over the standard τ_E of 1 ms [8]. Note that the enhanced τ_E averages over small dynamo events (described in the next paragraph), which momentarily degrade confinement. Accompanying the improved energy confinement is a poloidal beta $\equiv$ (plasma thermal pressure)/(edge poloidal magnetic pressure) of $\geq$ 7%. The particle confinement time is unknown due to uncertainty in the particle source rate, but low H_α (or D_α) radiation and a constant or rising $<n_e>$ indicate that particle confinement likely improves.

Referring again to Fig. 1, one observes sawtooth crashes throughout the discharge on the left and occasionally in the discharge on the right. In addition to appearing in the Ohmic input power and edge impurity emission, they also appear in the surface

poloidal voltage [Figs. 1(d) and 1(h)], which increases in response to an increase in the toroidal flux in the plasma volume. Thus, sawtooth crashes are dynamo events, characterized by the generation of poloidal plasma current and toroidal flux. During periods of enhanced confinement, dynamo events occur with substantially lower amplitude than sawtooth crashes [8]. These small dynamo events appear as rapid bursts in Figs. 1(f) and 1(h).

Most of the data discussed in the remainder of this Letter was gathered using probes inserted into the edge of MST plasmas with I_ϕ = 200 kA and $\langle n_e \rangle \sim 5 \times 10^{12}$ cm^{-3}. Magnetic sensing probes were used to measure $\boldsymbol{B}(r)$, and Langmuir probes were used to measure radial profiles of V_p (plasma potential), E_r (radial electric field) = $-\nabla(V_p)$, and V_f (floating potential). V_p was measured using the swept probe technique. On each of the Langmuir probes a shield was installed to block the small population of superthermal (fast) electrons present in the plasma edge [1]. Fast electrons can render the probe signals unreliable (e.g., from the sudden onset of thermionic electron emission) and lead to rapid destruction of the probes. Comparisons of Langmuir probe data with and without the shield show that its presence does not significantly affect the shape of the equilibrium profiles. Each data point in the profiles presented below is an ensemble average of time-averaged data from 10-30 similar discharges. The time windows are of varying length, chosen to avoid sawtooth crashes but averaging over small dynamo events in the enhanced confinement case. Error bars represent the statistical variation in the ensemble averages.

The radial electric field and its shear are relatively small in standard (low confinement) discharges, but both become large in a narrow region in the edge of enhanced confinement discharges. The profiles of $V_p(r)$ and $E_r(r)$ for both cases are shown in Figs. 2(a) and 2(b). The shear in the magnetic field is relatively weak in the plasma edge, so $E_r(r)$ approximates the shape of the sheared $\boldsymbol{E} \times \boldsymbol{B}$ flow profile. The positive E_r (pointing out of the plasma) in the shear region is in contrast to the negative E_r typical of the shear region in tokamaks and other devices [6].

The reduction of electrostatic and magnetic fluctuations during a period of enhanced confinement is shown in Fig. 3. The floating potential measured 2 cm from the plasma edge is shown in Fig. 3(a), and in Fig. 3(b) is shown the normalized rms fluctuation in the poloidal magnetic field, b_{rms}, measured with an array of magnetic pickup coils at the plasma edge. Before and after the period of enhanced confinement, fluctuation levels are substantial, and confinement is degraded. The surface poloidal voltage is included in Fig. 3(c) to show the timing of the small dynamo events. Each event momentarily increases both electrostatic and magnetic fluctuations. This discharge is atypical in that the time between small dynamo events is relatively long, and the time-averaged electrostatic and magnetic fluctuation amplitudes are particularly low.

The dominant contributors to b_{rms} are core-resonant global tearing modes with poloidal mode number $m = 1$ and toroidal mode numbers $n = 6$–10. Also important is the $(m,n) = (0,1)$ mode, resonant at the reversal radius (across which the toroidal field

changes direction) near the plasma edge. The (0,1) amplitude, and b_{rms}, increase momentarily with each small dynamo event [8]. A common feature of the $m = 1$ modes during enhanced confinement is that their normally steady growth between sawtooth crashes is absent [8]. In some discharges, like the one in Fig. 3, b_{rms} drops to ~ 1% between small dynamo events. This is close to the record low b_{rms} ~ 0.8% achieved recently in the MST when auxiliary poloidal current was driven in the edge plasma with the goal of reducing b_{rms} [4].

The reduction of electrostatic fluctuations during enhanced confinement occurs over the entire edge plasma and over a broad range of frequencies. This is illustrated in Fig. 4. The enhanced confinement and standard profiles of the total fluctuation power in the floating potential are shown in Fig. 4(a). These profiles result from frequency-integration over the ensemble power spectrum at each radius. Also shown is the enhanced confinement profile of E_r from Fig. 2(b). In addition to the roughly ten-fold reduction of fluctuation power over the entire edge plasma, the enhanced confinement profile also exhibits a further reduction in the region of strong shear. It is not known whether the weaker structure in the standard profile is physically significant. The power spectra comprising the total fluctuation power at 49 cm are shown in Fig. 4(b). Enhanced confinement spectra, comprising the total power inside the shear region (43.5 cm) and outside the shear region (45 cm), are shown in Fig. 4(c). In both cases, the reduction in fluctuation power occurs over the entire frequency range (1-250 kHz).

To summarize, RFP plasmas with increased energy and particle confinement are observed having a large, sheared radial electric field and reduced electrostatic and magnetic fluctuations. The electrostatic fluctuation power decreases ten-fold at all frequencies throughout the edge region ($r/a > 0.84$) and twenty-fold within the narrow ~ 1 cm region of strong shear at $r/a \approx 0.87$. The magnetic fluctuations are reduced to a level approaching the minimum ever observed in the MST.

The mechanisms underlying the electrostatic fluctuation reductions are not yet identified. The decrease in high frequency fluctuations within the region of strong shear is qualitatively consistent with existing theory [13], but this theory does not account for the decrease of low frequency fluctuations, which have correlation lengths ~ 10 cm [14], substantially larger than the width of the shear region. If the observed reductions result from the sheared flow implied by the sheared radial electric field, these observations could significantly extend the applicability of the sheared-flow turbulence suppression paradigm [13].

Improved confinement from reduced magnetic fluctuations in the RFP is anticipated, owing to the measured dominance of magnetic-fluctuation-induced transport [1,2]. The reduction of $m = 1$ magnetic fluctuations could result from the quasilinear edge current profile modification that occurs with each of the dominantly $m = 0$ small dynamo events, in analogy with auxiliary poloidal current drive [15,4]. However, the dramatic reduction in electrostatic turbulence might also affect energy transport. Further measurements are required to understand the relative importance of

electrostatic and magnetic fluctuations in these enhanced confinement discharges.

The authors are grateful to A. F. Almagri, D. Craig, and the MST group for help with data acquisition and to G. Fiksel, D. J. Den Hartog, and P. W. Terry for useful discussions. This work was supported by the U. S. Department of Energy.

[1] M. R. Stoneking *et al.*, Phys. Rev. Lett. **73**, 549 (1994).

[2] G. Fiksel *et al.*, Phys. Rev. Lett. **72**, 1028 (1994).

[3] J. S. Sarff *et al.*, Phys. Rev. Lett. **72**, 3670 (1994).

[4] J. S. Sarff *et al.*, Phys. Rev. Lett. **78**, 62 (1997).

[5] T. D. Rempel *et al.*, Phys. Rev. Lett. **67**, 1438 (1991).

[6] R. J. Groebner, Phys. Fluids B **5**, 2343 (1993).

[7] K. H. Burrell, Plasma Phys. Controlled Fusion **36**, A291 (1994).

[8] B. E. Chapman *et al.*, Phys. Plasmas **3**, 709 (1996).

[9] R. N. Dexter *et al.*, Fusion Tech. **19**, 131 (1991).

[10] Y. Hirano *et al.*, Nucl. Fusion **36**, 721 (1996).

[11] D. J. Den Hartog *et al.*, J. Nucl. Mater. **200**, 177 (1993); D. J. Den Hartog and R. D. Kendrick, *ibid.* **220-222**, 631 (1995).

[12] S. Hokin *et al.*, Phys. Fl. B **3**, 2241 (1991).

[13] H. Biglari, P. H. Diamond, and P. W. Terry, Phys. Fluids B **2**, 1 (1990).

[14] D. Craig (private communication).

[15] Y. L. Ho, Nucl. Fusion **31**, 341 (1991).

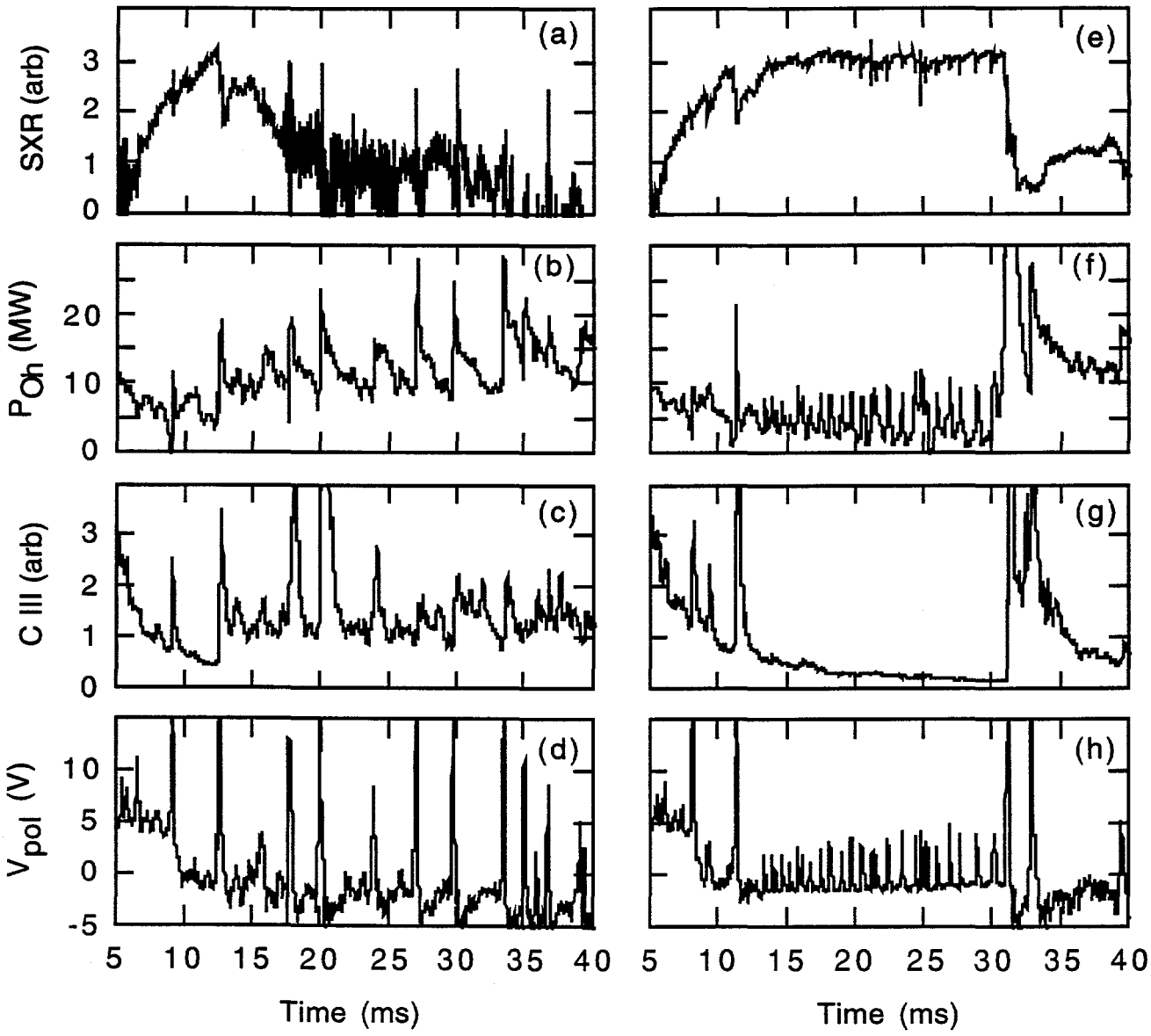

FIG. 1. Time variations of (a) ratio of two soft x-ray signals $\propto$ core electron temperature, (b) Ohmic input power, (c) *CIII* (464.74 nm) radiation, and (d) surface poloidal voltage in a standard discharge. These same parameters are shown in (e)-(h) for an enhanced confinement discharge.

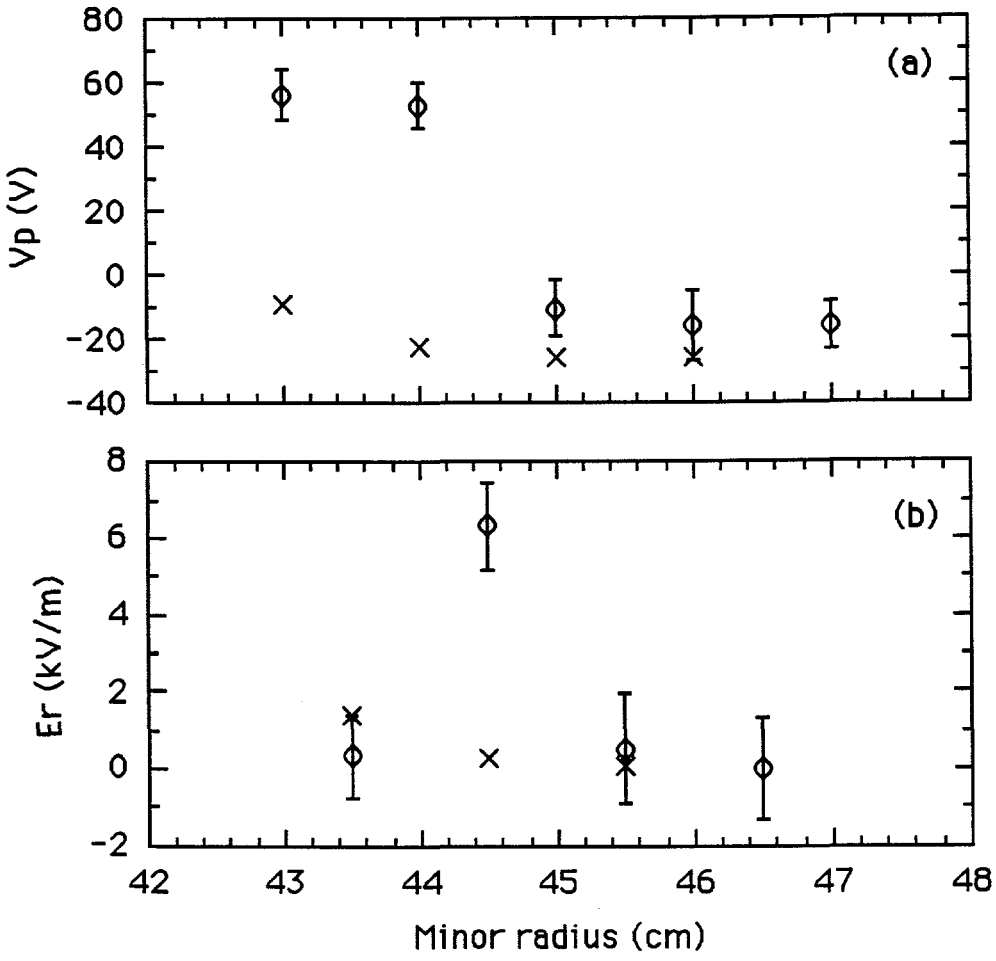

FIG. 2. Enhanced confinement (o) and standard (x) profiles of (a) plasma potential and (b) radial electric field. Here, "standard" refers to discharges with relatively weak reversal ($F \sim -0.2$). Error bars are shown only for the enhanced confinement data, but error bars for the standard data are similar.

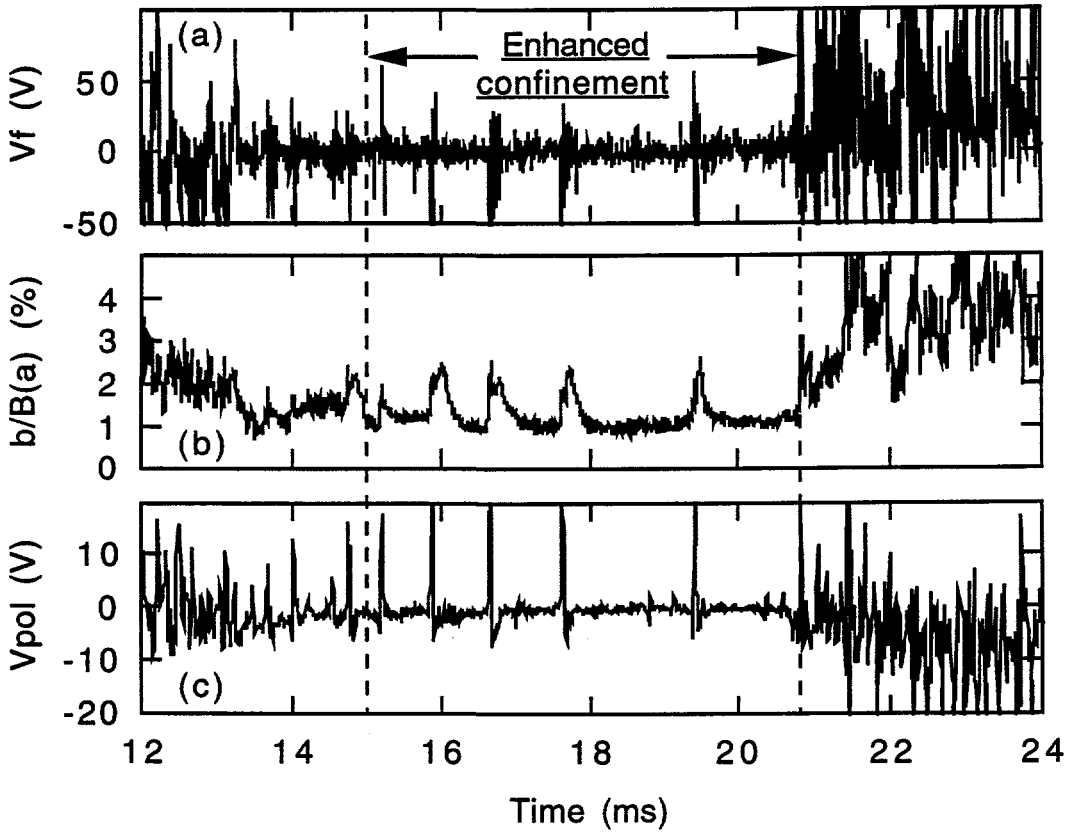

FIG. 3. Time variations of (a) floating potential 2 cm from the plasma edge, (b) rms fluctuation in the poloidal magnetic field normalized to the total field at the edge, and (c) surface poloidal voltage during a discharge with a period of enhanced confinement.

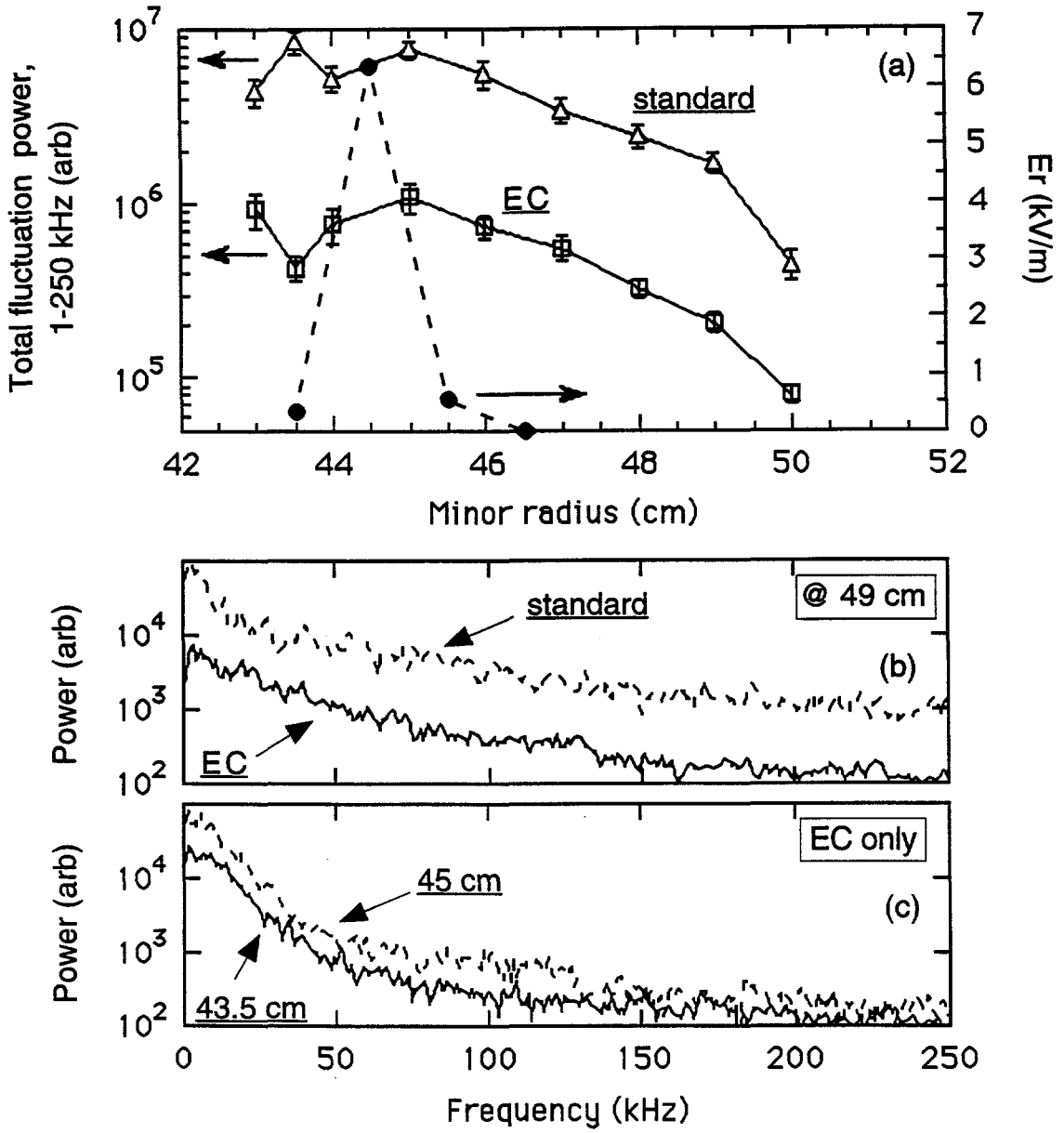

FIG. 4. (a) Profiles of the enhanced confinement (EC) radial electric field and total fluctuation power in the floating potential, (b) enhanced confinement and standard power spectra at 49 cm, and (c) enhanced confinement power spectra at 43.5 cm and 45 cm. Spectra are frequency-integrated to derive the total fluctuation power in (a). Here, "standard" refers to low confinement periods of strongly reversed discharges.

EXTERNAL DISTRIBUTION IN ADDITION TO UC-20

S.N. Rasband, Brigham Young University
R.A. Moyer, General Atomics
J.B. Taylor, Institute for Fusion Studies, The University of Texas at Austin
E. Uchimoto, University of Montana
F.W. Perkins, PPPL
O. Ishihara, Texas Technical University
M.A. Abdou, University of California, Los Angeles
R.W. Conn, University of California, Los Angeles
P.E. Vandenplas, Association Euratom-Etat Belge, Belgium
Centro Brasileiro de Pesquisas Firicas, Brazil
P. Sakanaka, Institute de Fisica-Unicamp, Brazil
Mme. Monique Bex, GANIL, France
J. Radet, CEN/CADARACHE, France
University of Ioannina, Greece
R. Andreani, Associazione EURATOM-ENEA sulla Fusione, Italy
Biblioteca, Istituto Gas Ionizzati, EURATON-ENEA-CNR Association, Italy
Plasma section, Energy Fundamentals Division Electrotechnical Laboratory, Japan
Y. Kondoh, Gunma University, Kiryu, Gunma, Japan
H. Toyama, University of Tokyo, Japan
Z. Yoshida. University of Tokyo, Japan
FOM-Instituut voor Plasmafysica "Rijnhuizen," The Netherlands
Z. Ning, Academia Sinica, Peoples Republic of China
P. Yang, Shandong University, Peoples Republic of China
S. Zhu, University of Science & Technology of China, People's Republic of China
I.N. Bogatu, Institute of Atomic Physics, Romania
M.J. Alport, University of Natal, Durban, South Africa
R. Storer, The Flinders University of South Australia, South Australia
B. Lehnert, Royal Institute of Technology, Sweden
Librarian, CRPP, Ecole Polytechnique Federale de Lausanne, Switzerland
B. Alper, Culham Laboratory, UK
A. Newton, UK

2 for Chicago Operations Office
5 for individuals in Washington Offices

INTERNAL DISTRIBUTION IN ADDITION TO UC-20
80 for local group and file